

Estimation of IASCC Initiation Susceptibility of Proton-irradiated Stainless Steels by IG Cracks Analysis on Irradiated Cross-sectional Area

Ju-Eun Park ^{a,b}, Dong-Jin Kim ^a, Min-Jae Choi ^{a*}, Dong-Bok Lee ^b

^a Nuclear Material Research Division, Korea Atomic Energy Research Institute,
111 Daedeok-daero-989, Yuseong-gu, Daejeon 34057

^b Department of advanced Material Science & Engineering, Sungkyunkwan University, Suwon, Korea

*Corresponding author: mjchoi@kaeri.re.kr

1. Introduction

The main role of reactor internals in the PWR is to maintain the geometric integrity of the reactor core and to support the fuel rod. Most of these internal structures are made of stainless steels. Type 304 or 316 stainless steels are used for the reactor internals, they have several degradation mechanisms under the primary water condition with high neutron fluence. Irradiation assisted stress corrosion cracking (IASCC) is one of the most important degradation mechanism. The failure of baffle-former bolt in the reactor internals has been reported in many countries, the reason of failure has generally been evaluated to IASCC. In this study, we tried to develop the method of quantification of IASCC initiation susceptibility by analyzing the intergranular cracks which are occurred on the irradiated cross-sectional area after the slow strain rate test (SSRT) with 10% strain.

2. Methods and Results

2.1 Materials and Specimens preparation

The material used in the experiments was type 316 stainless steel. The chemical composition is shown in table 1.

Cr	Ni	P	Mo	Mn	
16.7	10.8	0.05	2.0	1.3	
Si	S	C	Fe		wt%
0.59	0.001	0.047	Bal.		

Table 1. Chemical composition of type 316 stainless steel

The specimens were made by electric discharge machining (EDM) for SSRT like Fig 1.

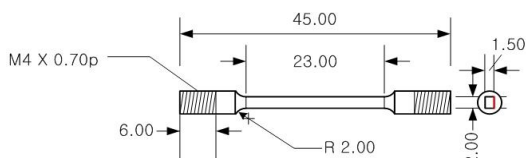


Fig. 1. SSRT test specimen

Irradiation of specimens was performed by using 2.0 MeV protons in General Ionex Tandetron accelerator at the Michigan Ion Beam Laboratory (MIBL). Irradiations were conducted at 40 μ A of current to 1, 3, 5 and 10 dpa by controlling irradiation time. The proton implantations (Fig. 2) and the irradiation doses (Fig. 3) for the each irradiation sample were calculated by using SRIM code with considering the irradiation conditions.

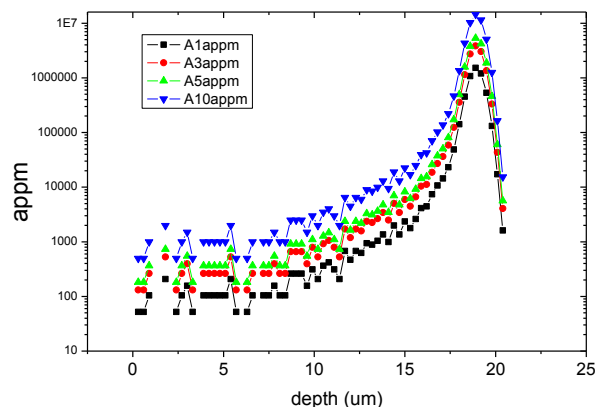


Fig. 2. Proton implantations calculated by SRIM code

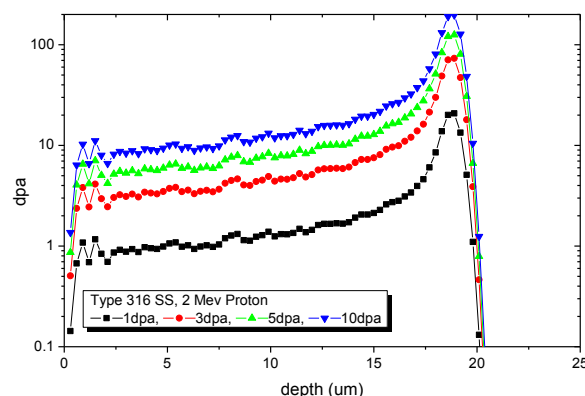


Fig. 3. Irradiation doses calculated by SRIM code

Proton irradiation area for the samples was observed by scanning electron microscope (SEM) like Fig 4. Irradiation depth could be measured by observing the irradiation band around 20 μ m of depth. Maximum irradiation doses were calculated on around 20 μ m by SRIM code, the observed irradiation depth values had a

good agreement with the expected results by the calculation.

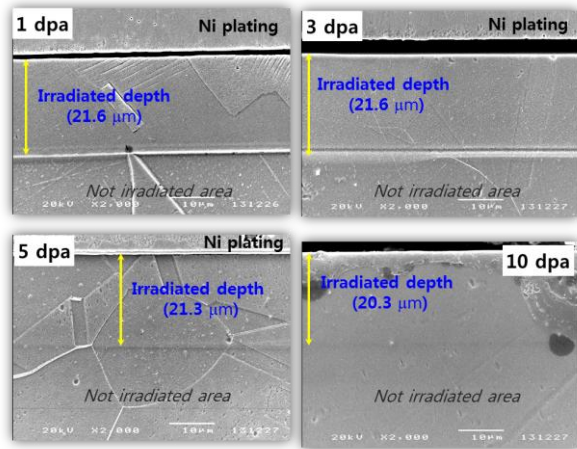


Fig. 4. Irradiation depth observed by SEM

2.2 SSRT

SSRT were carried out in the autoclave under the simulated primary water conditions which were 1200 ppm of B, 2 ppm of Li, 6 ~ 6.5 of pH, 21.2 ~ 21.5 $\mu\text{S}/\text{cm}$ of conductivity and under 5 ppb of dissolved oxygen. The strain rate was $3.4 \times 10^{-7}/\text{s}$ and the samples were strained to 10 %. The temperature and pressure were 325°C and 165 bar in autoclave. The conditions with the dissolved hydrogen (DH) were 25 and 50 cc/kg·H₂O to estimate the effect of DH concentration on IASCC initiation.

2.3 Sample preparation

Fig. 5 shows one of the specimens taken after slow strain rate tests. In this study, we have developed the method of specimen preparation to investigate how the cracks progress on the cross section to the depth direction rather than cracks at the irradiated surface as follows below. The cutting position is shown in Fig. 5 in order to observe the microstructure of the cross-sectional surface.

The specimens were cut through the microfabrication process with a length of 7 mm including the non-irradiated area from the middle of the sample. The two pieces obtained after cutting were schematized (Fig. 6) and then these were rotated 90 degrees so that the irradiated surfaces were faced each other. After that, the cross-sectional area faces downward and two pieces of the proton-irradiated surface were attached using G1 epoxy as being the ratio of resin to hardener is 10:1. After sufficient time for the epoxy was completely harden, it was mounted with a light curing machine.

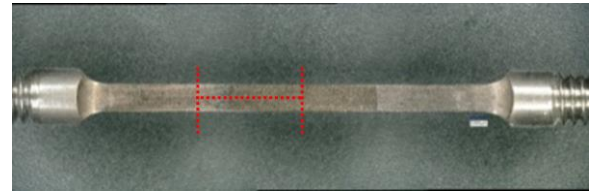


Fig. 5. Cutting position

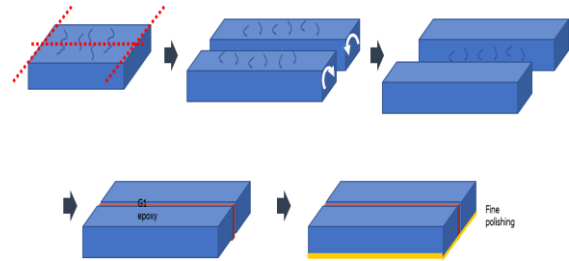


Fig. 6. Mounting process for observing Cross-sectional area

2.4 Cross-sectional area images

As a result, Figs. 7 and 8 are pictures of mounting specimens taken by a visible light microscope (VLM) and a scanning electron microscope (SEM). The pictures are classified according to the conditions of dissolved hydrogen concentration and irradiation doses. Figs. 7 (a) and (b) show the results for each dose at 25cc/kg·H₂O DH condition and Figs. 8 (a) and (b) show the results for each dose at 50cc/kg·H₂O DH condition.

At the same hydrogen concentration condition, as the irradiation dose increase, the number of cracks are much larger and the size of the cracks increases. It can be seen that as the dose increase, the crack initiation susceptibility increases significantly. Moreover, the crack size and the number of cracks were increased at 50cc/kg·H₂O DH condition than 25cc/kg·H₂O DH condition and it indicated that the susceptibility of crack initiation is related to dissolved hydrogen concentration and dose.

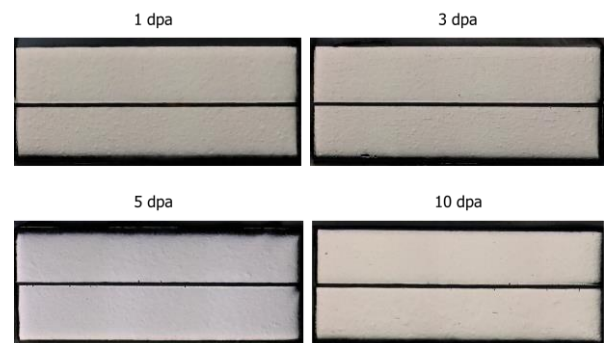
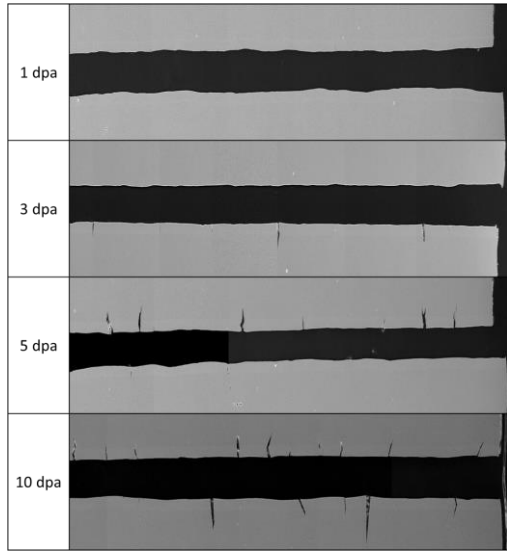


Fig. 7. (a) The VLM images on cross-sectional area of 25cc/kg·H₂O DH condition



(b) The SEM images on cross-sectional area of 25cc/kg·H₂O DH condition

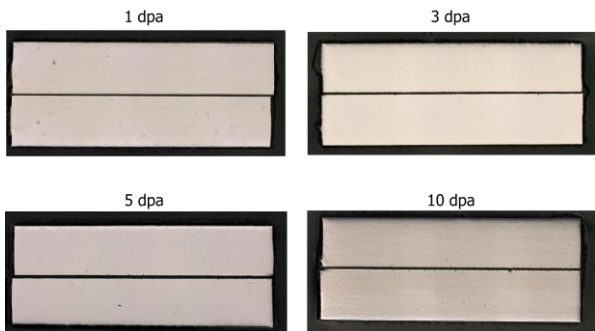
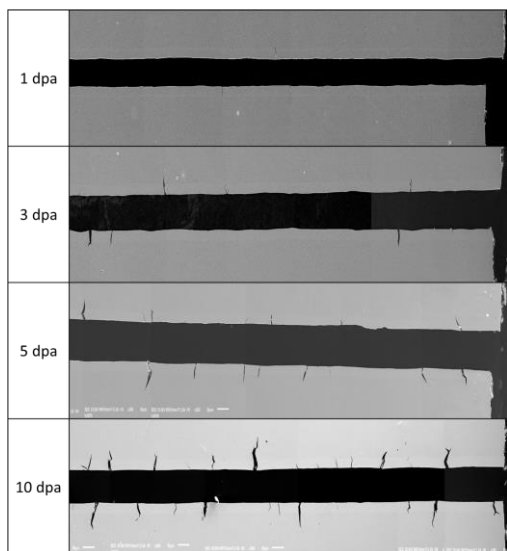


Fig. 8. (a) The VLM images on cross-sectional area of 50cc/kg·H₂O DH condition



(b) The SEM images on cross-sectional area of 50cc/kg·H₂O DH condition

2.5 Crack Number Density on Cross-sectional Area (in proton irradiated area)

To calculate the crack initiation susceptibility quantitatively under each condition, the crack number density, which commonly counts the intergranular (IG) cracks on the surface, was applied to calculate crack number density on the cross-sectional area in proton irradiated area. It is calculated by the number of cracks was divided by the proton-irradiated area. In other words, the proton-irradiated area was calculated as the same with the width of the specimen multiplied by the irradiation area multiplied by 2 pieces. The values of crack number density were fitted using the above method and it is shown as Fig. 9.

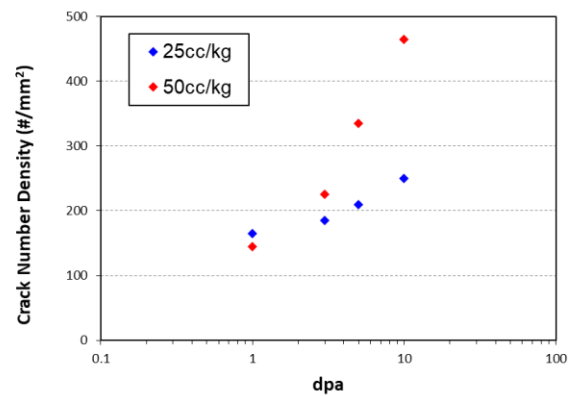


Fig. 9. Crack number density on cross-sectional area

3. Conclusions

The slow strain rate tests were performed using the proton irradiated 316 stainless steels at the simulated primary water conditions. We had prepared the cross sectional specimens to observe how the stress corrosion cracking generated on the surface were forming material inside. From an above results, it was confirmed that the cracks generated along the grain boundary on the surface were propagated along grain boundary inside as well. As the dose increased, the crack initiation susceptibility increased and the crack initiation susceptibility depending on the hydrogen concentration showed a high crack density under the condition of 50cc/kg·H₂O compared to dissolved hydrogen concentration of 25cc/kg·H₂O. Therefore IASCC initiation susceptibility was increased by increasing irradiation doses and by increasing DH concentration.